Fluorescence Properties of the $Ru(bpy)_3^{2+}$ Complex Incorporated in Sol−Gel-Derived Silica Coating Films

Plinio Innocenzi,† Hiromitsu Kozuka,* and Toshinobu Yoko

Institute for Chemical Research, Kyoto University, Uji, Kyoto-Fu 611, Japan

Received: December 17, 1996[⊗]

Silica gel coating films doped with $Ru(bpy)_3^{2+}$ complexes were prepared by the sol−gel method from a hydrolyzed tetraethoxysilane solution containing $[Ru(bpy)_3^{2+}]Cl_2 \cdot 6H_2O$. UV−visible optical absorption spectra, fluorescence emission spectra, fluorescence efficiency and lifetime, and infrared absorption spectra were measured for the films dried at various temperatures. The fluorescence band attributed to the transition from the metal-to-ligand charge transfer excited state to the ground state of $Ru(bpy)_3^{2+}$ was found to show blue shift on sol-to-gel film conversion, red shift with increasing drying temperature up to 200 °C, and then blue shift again over 200 °C. The fluorescence lifetime increased and the fluorescence efficiency decreased with increasing drying temperature. In the as-deposited film, the complexes are thought to be surrounded by the solvent molecules which interact with the silanol groups of the gel network so strongly that the Franck−Condon excited state of the complex may be relaxed to a less extent, giving rise to the blue shift of the fluorescence peak on the sol-to-gel film conversion. During drying up to 200 °C the solvent in the gel pores evaporates, leaving the gel pores filled with air; the complexes are just weakly interacting with the gel network, obtaining more freedom of rotation and surrounded by air molecules, which results in the red shift of the fluorescence peak. Over 200 °C, the gel pores start to collapse and the complexes are immobilized in the gel network, strongly interacting with and fully surrounded by the silanol groups and/or siloxane chains, which is reflected in the blue shift of the fluorescence peak.

1. Introduction

Ruthenium complexes are among the most widely studied organometallic molecules in recent years because of their variety of attractive functions based on luminescence properties with a long excited state lifetime, redox properties, and excited state reactivities and relatively high chemical and thermal stability. Such unique features make the ruthenium complex doped materials quite attractive as optical sensors,[1−4] photocatalysts,[5] photoelectrodes for solar cells,[6,7] and nonlinear optical materials.[8]

Entrapping ruthenium complexes in solid matrices, particularly in thin films, allows the preparation of devices for many applications. The sol−gel technique is especially suitable for preparing inorganic oxide thin films doped with functional organic molecules and organometallic complexes,[9−11] where metal alkoxide solutions containing dopants are used as the starting materials. So far ruthenium complexes have been reported to be successfully incorporated in inorganic oxide thin films[4,9,12] as well as in oxide bulk gels,[13−15] and applications in devices such as optical sensors[2−4] have been demonstrated.

Many of the previous works on doped sol−gel materials have demonstrated that the dopants are present as an individual molecule or complex in the inorganic matrices, retaining their properties in the matrices as in the solution states. In other words, the functionality of the dopants are also available in the solid state, which allows the doped materials to be used as devices. We have to recognize, however, that the mesoscopic structure and chemical nature of gel matrices change in the drying stage, where the incorporation of the dopants proceeds; the solvent evaporation, the further condensation reaction between the hydroxyl groups of the inorganic network, and the gel pore shrinkage occur in the drying stage. These changes in the structure and chemistry of the gel matrix should affect the state of the dopants, which causes the change in the dopant properties. In fact, in our previous work on the change of the optical properties of rhodamine 6G (Rh6G) doped silica gel films,[16] we have found that the Rh6G's are present as monomers in the precursor sols, changed into dimers in the as-deposited films and changed gradually into monomers during drying up to 150 °C. We have attributed the dimerization in the as-deposited films and the monomerization during drying to the increased concentration of the Rh6G molecules in the gel pores and the increased interaction between the Rh6G molecules and the silanol groups, respectively. These experimental facts and consideration suggest that the optical properties of the organic or organometallic dopants should be controlled with recognizing the state of the dopants, which is changed during the drying process via changes in the structure and chemical nature of the gel matrix.

In order to control and optimize the optical, photochemical, and photoelectrochemical functions of ruthenium complex doped sol−gel thin films, it is of importance to have knowledge on how the properties of the complex are changed in the incorporation process. From this point of view we have focused our attention on the changes of the optical properties of tris(2,2′-bipyridyl)ruthenium(II), $Ru(bpy)_3^{2+}$, entrapped in silica gel films under drying in the present work. Besides the importance of the ruthenium complexes as the functional dopants, they have an advantage for studying the process of incorporation because they are stable up to relatively high temperatures, which allows us to monitor the change of their state up to high drying temperatures.

2. Experimental Section

Precursor sols were prepared from a solution containing tetraethoxysilane (TEOS), $Si(OC_2H_5)_4$ (Shinetsu Chemicals), 1N

* Corresponding author. E-mail: kozukahr@scl.kyoto-u.ac.jp.
† On leave from Dipartimento di Ingegneria Meccanica, Sezione Materiali, Università di Padova, Via Marzolo 9, 35131 Padova, Italy.
⊗ Abstract published in *Advance ACS Abstracts,* March 15, 1997.

S1089-5647(97)00004-7 CCC: $14.00

HCl (Nacalai Tesque), ethanol (EtOH) (Wako Pure Chemicals Industries), and deionized water. The mole ratios H_2O/TEOS and HCl/TEOS were 4 and 0.01, respectively. The amount of EtOH was selected so that the solutions had an equivalent SiO_2 concentration of 100 g L^{-1}. The starting solution was prepared by adding the aqueous solution of HCl containing a half of the prescribing amount of water dropwise to the ethanolic solution of the alkoxide, and then two hours later the other half of the water amount was added. The solution was kept standing at room temperature under stirring for 4 h. Then tris(2,2′-bipyridyl)ruthenium(II) chloride hexahydrate, $[Ru(bpy)_3]Cl_2 \cdot 6H_2O$ (Aldrich), was dissolved in the sol, which was further stirred at room temperature for 30 min. The concentration of $Ru(bpy)_3^{2+}$ in the sol was 5×10^{-3} M. During the preparation, the solutions were sealed and kept in the dark.

Coating films were prepared from the sol by dip-coating on a cleaned sodalime silicate glass slide substrate (Matsunami Glass Industries) at a withdrawing rate of 7.5 cm min^{-1}. After the deposition, the films were dried in an oven in air at 50, 100, 150, 200, 250, and 300 °C, successively. The films were dried at each temperature for 10 min.

Optical absorption spectra of the coating films were measured in the range 200−800 nm by a Hitachi U-3500 spectrophotometer with a resolution of ±1 nm. A sodalime silicate glass slide was used as a reference. The thickness of the coating films was measured by a Kosaka Laboratory SE-30 D profilometer. The thickness of the as-deposited film was 0.28 μm.

Infrared absorption spectra were measured in the range 400−4500 cm^{-1} by a Fourier transform infrared (FTIR) spectrophotometer (Model FTIR-5M, Japan Spectroscopic Co.) with a resolution of ±4 cm^{-1}. Films deposited on silicon wafers were used for this purpose. The silicon wafers were p-type ⟨100⟩, polished on one face and 0.7 mm in thickness.

Fluorescence spectra were obtained by a Hitachi 850 fluorescence spectrophotometer. The emission spectra were obtained using an excitation wavelength of 440 nm. Relative fluorescence efficiency was determined by dividing the area of the fluorescence spectra by the absorbance at 440 nm.

Emission anisotropy, r, in the $Ru(bpy)_3^{2+}$ doped silica films was measured at a wavelength of 603 nm. The measurements were done using two pieces of polarizers placed at the excitation and emission sides with parallel or perpendicular configurations. The value of anisotropy r was calculated as

$$r = \frac{I_{VV} - GI_{VH}}{I_{VV} + 2GI_{VH}} \quad (1)$$

where the subscripts V and H indicate vertical and horizontal configurations of the polarizers, respectively, and the first and second subscripts correspond to the polarizers placed at the excitation and emission sides, respectively.[14] The G factors were defined by eq 2, which account for the different sensitivity of the detection system to vertically and horizontally polarized light.[14]

$$G = \frac{I_{HV}}{I_{HH}} \quad (2)$$

Fluorescence decay parameters were determined by a single-photon counting method on a Horiba NAES-550 using a hydrogen flash lamp as the exciting light.

Differential thermal analysis (DTA) and thermogravimetric analysis (TG) were carried out in air at a rate of 10 °C min^{-1} for the $[Ru(bpy)_3]Cl_2 \cdot 6H_2O$ reagent using a Netzsch STA 409/429 thermal analyzer.

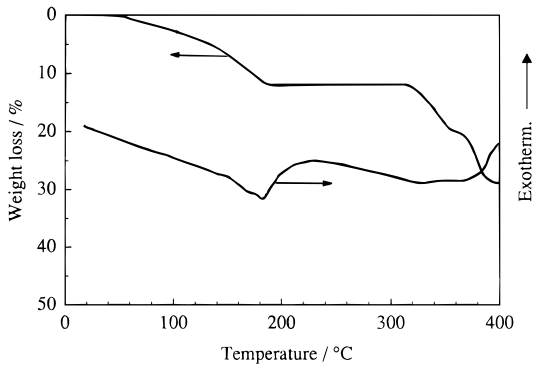

Figure 1. DTA and TG curves of the $[Ru(bpy)_3]Cl_2 \cdot 6H_2O$ reagent measured at a rate of 10 °C min^{-1} in air.

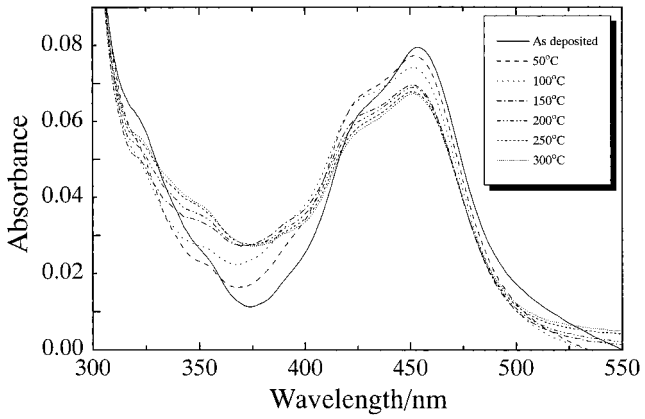

Figure 2. Optical absorption spectra of the silica gel films doped with $Ru(bpy)_3^{2+}$ and dried at different temperatures.

3. Results

3.1. DTA and TG Curves of $[Ru(bpy)_3]Cl_2 \cdot 6H_2O$. Figure 1 shows the DTA and TG curves of the $[Ru(bpy)_3]Cl_2 \cdot 6H_2O$ reagent. A weight loss of 12% was observed up to 190 °C, accompanied with an endothermic peak. Because the mass fraction of H_2O in $[Ru(bpy)_3]Cl_2 \cdot 6H_2O$ is calculated to be 14%, the weight loss observed up to 190 °C can be attributed to the dissociation of the crystal water from the $[Ru(bpy)_3]Cl_2 \cdot 6H_2O$.

No weight loss was observed from 190 to 320 °C. If a ligand exchange reaction $[Ru(bpy)_3]Cl_2 \rightarrow [Ru(bpy)_2Cl_2] + bpy$ occurs, there should be a weight loss of 21%, which was not observed in the present TG curve. Therefore, it can be concluded that the $[Ru(bpy)_3]^{2+}$ complex is thermally stable at least up to 320 °C.

3.2. Optical Absorption Spectra. Figure 2 shows the optical absorption spectra of the $Ru(bpy)_3^{2+}$ doped silica gel coatings dried at different temperatures. The absorption spectra of $Ru(bpy)_3^{2+}$ doped samples (Figure 2) showed an intense absorption band at 450 nm and a shoulder at 420 nm, which are both assigned to metal-to-ligand charge transfer (MLCT) (t_{2g} (Ru) → π^* (bpy) transitions), and smaller bands or shoulders at 325 and 350 nm, which are assigned to metal centered (MC) d−d transitions.[17−21] [The shoulder at 420 nm is originated from the splitting of the energy level of the first excited state into two separate levels caused by the trigonal symmetry of the complex.[17,19] An intense band at 285 nm (not shown in the figures) is attributed to ligand centered ($\pi \rightarrow \pi^*$) transitions. The excited states of the metal centered transitions have singlet−triplet mixing because of the spin−orbit coupling effect.[21]] The absorbance at 450 nm slightly decreased with increasing drying temperature up to 150 °C, and above this temperature the spectra showed no substantial change. It should be noted that no shift in the absorption maxima was observed throughout the sol-to-

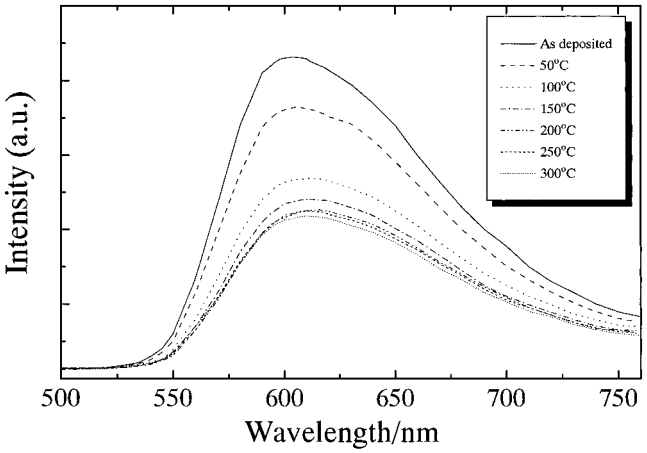

Figure 3. Fluorescence emission spectra of the silica gel films doped with $Ru(bpy)_3^{2+}$ and dried at different temperatures.

gel film conversion and drying process. It should also be pointed out that the 350 nm MC band increased with increasing drying temperature without changing the position.

3.3. Fluorescence Spectra. The fluorescence spectra of the $Ru(bpy)_3^{2+}$ doped films and the dependence of the fluorescence peak position on drying temperature are shown in Figures 3 and 4, respectively. The fluorescence maxima observed at 600−620 nm are attributed to emission from the triplet MLCT excited state (^{3}MLCT) to the ground state.[17] A significant decrease in the fluorescence intensity was observed with increasing drying temperature up to 100 °C, whereas a small decrease was observed above this temperature, which is more clearly depicted in Figure 5. As seen in Figure 4, the fluorescence peak showed a blue shift from 620 to 603 nm when the precursor sol was converted into the as-deposited gel film. A red shift was then observed with increasing drying temperature up to 200 °C, and a blue shift was observed again at higher temperatures.

The emission anisotropy r of the as-deposited film was estimated to be 0.08 (±0.02). The samples dried at higher temperatures gave unreliable values because of the much lower fluorescence intensities.

3.4. Fluorescence Lifetime. The fluorescence decay data for the present coating films could not be fit to a single-exponential curve. As shown in Figure 6, the fluorescence decay data could be fit very well to a biexponential decay curve expressed by[14]

$$I(t) = \sum_{i=1}^{2} \alpha_i \exp[-(t/\tau_i)] \qquad (3)$$

where $I(t)$ represents the fluorescence intensity at time t, τ_i the decay time, and α_i the preexponential factor. The weighted mean lifetimes were calculated by:[14]

$$\langle\tau\rangle = \sum_{i=1}^{2} \alpha_i \tau_i^2 / \sum_{i=1}^{2} \alpha_i \tau_i \qquad (4)$$

The results of the lifetime measurements are summarized in Table 1. The average lifetime was found to increase abruptly with increasing drying temperature, especially up to 100 °C.

3.5. Infrared Spectra. Figure 7 shows the infrared absorption spectra of the undoped films dried at different temperatures. Three peaks characteristic of the Si−O bond are observed: the bands at 1070 and 800 cm^{-1} attributed to the antisymmetric and symmetric stretching vibration of the Si−O bonds, respectively, and that at 450 cm^{-1} to the rocking vibration of Si−O−Si bonds.[22] The peak at 910−940 cm^{-1} is attributed to the

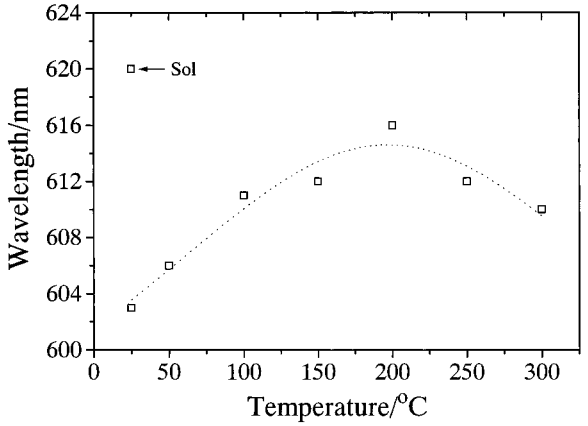

Figure 4. Fluorescence emission peak position as a function of drying temperature for the silica gel films doped with $Ru(bpy)_3^{2+}$ and the sol.

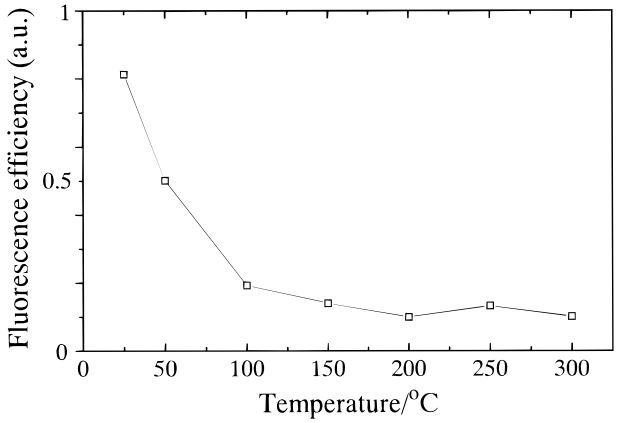

Figure 5. Relative fluorescence efficiency as a function of drying temperature for the silica gel films doped with $Ru(bpy)_3^{2+}$.

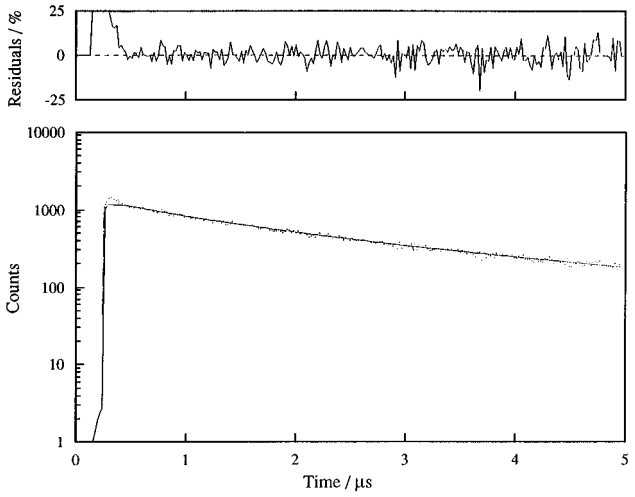

Figure 6. A fluorescence emission decay curve for the silica gel films doped with $Ru(bpy)_3^{2+}$ and dried at 100 °C. Residuals to the fit are also shown to evaluate the fitting quality.

stretching vibrations of Si−OH and Si−O^- bonds.[23] The broad band around 3400 cm^{-1} is assigned to the stretching vibration of O−H groups.[24] The relative variations of the 910−940 cm^{-1} and 3400 cm^{-1} band areas are shown in Figure 8 as a function of drying temperature. For the 910−940 cm^{-1} band, a little decrease was observed with increasing drying temperature up to 100 °C, followed by a plateau up to around 200 °C and an abrupt decrease at higher temperatures. A marked decrease was observed for the 3400 cm^{-1} band area at 100 °C and a slight decrease was seen above 100 °C.

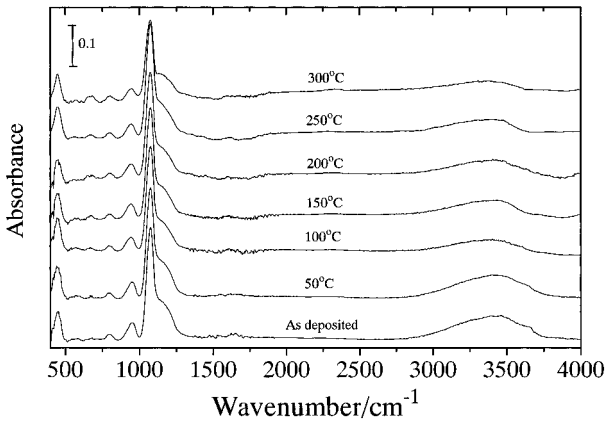

Figure 7. Infrared absorption spectra of the undoped silica gel films dried at various temperatures.

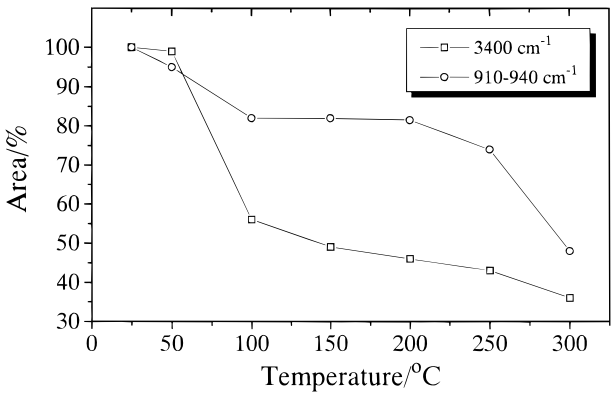

Figure 8. Variation of the 910−940 and 3400 cm^{-1} infrared absorption band area as a function of drying temperature for the undoped silica gel films.

TABLE 1: Fluorescence lifetime data for the silica gel films doped with $Ru(bpy)_3^{2+}$ and dried at different temperatures

	lifetime (μs)			preexponential term	
drying temp (°C)	τ_1	τ_2	$\langle\tau\rangle$	α_1	α_2
as-deposited	0.841	0.124	0.829	0.0621	0.0092
100	3.18	0.596	1.81	0.0028	0.0179
200	3.31	0.541	2.44	0.0027	0.0076
300	3.34	0.691	2.16	0.0029	0.015

4. Discussion

4.1. Thermal Stability of the $[Ru(bpy)_3]^{2+}$ Complex. Gleria et al.[25] and Durham et al.[26] observed the optical absorption spectral change during the ligand exchange reaction $[Ru(bpy)_3]X_2 \rightarrow [Ru(bpy)_2X] + bpy$ (X: halide ion), which was allowed by irradiating the complex solution at 436 nm. They found that the 450 nm band decreases and a 550 nm band emerges with the ligand exchange reaction. Such a spectral change was not observed in the present gel films with increasing drying temperature. The thermal analysis data for the $[Ru(bpy)_3]Cl_2 \cdot 6H_2O$ reagent did not show any weight loss corresponding to the ligand exchange reaction at least up to 320 °C. Therefore the $[Ru(bpy)_3]^{2+}$ complex entrapped in the silica gel films can be concluded to be thermally stable up to the temperature that we employed in the present study.

4.2. Fluorescence Peak Shift. One can find many papers[14,15,27−33] dealing with the mechanism of the so-called "rigidochromism" originally termed by Wrighton and Morse;[27] $Ru(bpy)_3^{2+}$ emits light of longer wavelengths in a fluid solution than in a rigid matrix. The excited state of solvated $Ru(bpy)_3^{2+}$ is now believed to have an asymmetric charge distribution because of the single ligand-localized excitation, while the ground state has a symmetric charge distribution. In a fluid solution, the solvent molecules can quickly reorient after excitation of the complex to solvate the new, highly polar MLCT excited state; that is, the Franck−Condon (unrelaxed) excited state is thermally relaxed as schematically illustrated in Figure 9a. In other words, the excited state of the complex is stabilized relative to the ground state by the surrounding solvent dipoles, and the complex then emits light from a relaxed excited state. On the other hand, in a rigid matrix, because the solvent cannot reorient, the Franck−Condon (unrelaxed) excited state is not completely stabilized or relaxed within its lifetime, and hence the emission occurs from a higher energy level than that in a fluid solution. This leads to a blue shift in the emission when the surrounding media experience "fluid-to-glass transition" or freezing as illustrated in Figure 9a.

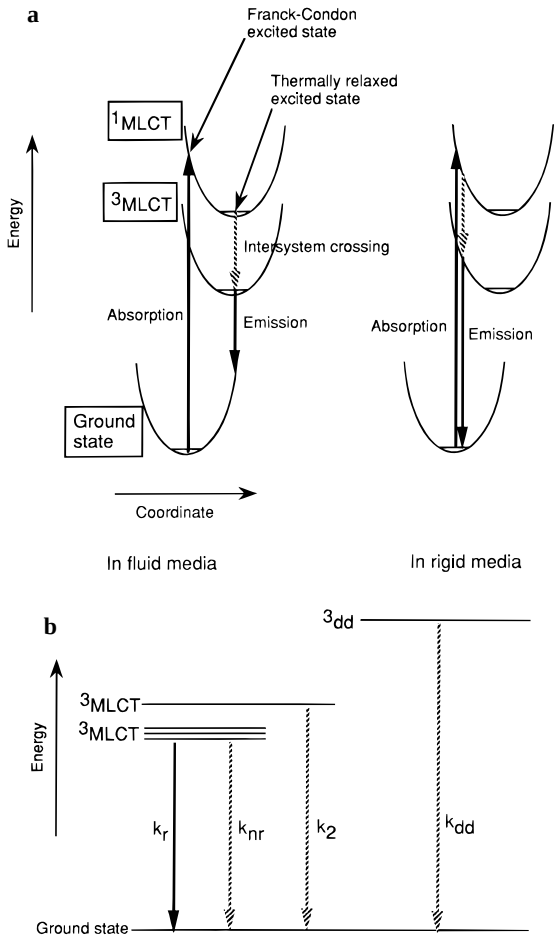

Figure 9. (a) Schematic illustration showing the energy vs nuclear configuration for the electronic transitions in the $Ru(bpy)_3^{2+}$ complexes. (b) Schematic illustration showing the excited state deactivation pathways (after ref 38).

In the present study, fluorescence peak shifts were detected on sol-to-gel film conversion and gel film drying (Figures 3 and 4), whereas no shift was observed in the absorption peak (Figure 2). This means that the change in the surrounding media affected only the relaxation of the MLCT excitation state without changing the Franck−Condon (unrelaxed) excited state. Blue shifts of the $Ru(bpy)_3^{2+}$ emission peak throughout sol-to-gel conversion and gel aging and drying processes is a well-known phenomenon in bulk silica or aluminosilicate gels,[14,15,29] and several authors attributed this blue shift to rigidochromism. In the present study, however, the emission peak did not show continuous blue shift throughout the overall process of sol-to-gel film conversion and drying. The emission peak showed blue shift on sol-to-gel film conversion, red shift with increasing

drying temperature up to 200 °C, and blue shift again at higher temperatures.

In the sol state, the $Ru(bpy)_3^{2+}$ complexes are surrounded by solvent molecules, which can easily reorient when $Ru(bpy)_3^{2+}$ is photoexcited and obtains a dipole moment. There are two possibilities for the state of the $Ru(bpy)_3^{2+}$ complexes in the as-deposited gel film; $Ru(bpy)_3^{2+}$ complexes are (1) still surrounded by solvent molecules or (2) completely entrapped in the gel network, namely, directly bonded to and fully surrounded by the silanol groups of the gel network. It is likely, however, that in the as-deposited film the $Ru(bpy)_3^{2+}$ complexes are still surrounded by solvent molecules, H_2O and C_2H_5OH, because the emission anisotropy values of about 0.08 are much lower than the limiting anisotropy of 0.4 expected when the transition moments are collinear.[14] This indicates that the $Ru(bpy)_3^{2+}$ complexes have a residual freedom of rotational motion. It should be noted, however, that the solvent molecules surrounding the $Ru(bpy)_3^{2+}$ complexes are not fully free to move or rotate because of their possible interaction with the silanol groups of the gel network. This restriction in the freedom of movement of the solvent molecules would cause the rigidochromism of the $Ru(bpy)_3^{2+}$ complexes, i.e., blue shift of the emission peak on sol-to-gel film conversion. The environment of the $Ru(bpy)_3^{2+}$ complexes can be said to experience the fluid-to-glass transition on sol-to-gel film conversion.

At higher temperatures one can expect further evaporation of the solvent, which results in an increase in direct interaction between the complexes and the silanol groups of the rigid gel network. This should lead to a blue shift of the emission, which is, however, opposite to what we observed with increasing drying temperature up to 200 °C. Possible explanations and arguments for the observed red shift are as follows.

(a) At first glance, the preferential evaporation of ethanol seems to be the origin of the red shift because the fluorescence maxima of $Ru(bpy)_3^{2+}$ in water was observed at a longer wavelength (627 nm) than that in ethanol (616 nm), and similar observation was reported in refs 1 and 18. However, although the infrared (IR) spectra of the present samples showed drastic evaporation of both water and ethanol up to 100 °C, the red shift of the emission peak continued to occur even above 100 °C. Therefore, the observed red shift apparently does not reflect the preferential evaporation of ethanol.

(b) Evaporation of the solvent increases the concentration of HCl in the gel pores. This would result in the increased number of $Si-OH_2^+$. Matsui et al.[15] observed a red shift of $Ru(bpy)_3^{2+}$ emission in bulk silica gels when a higher HCl concentration was employed in the precursor solution. They attributed the red shift to the decreased electrostatic interaction between the complexes and the silanol groups; $Ru(bpy)_3^{2+}$ complexes are less strongly attached to silanol groups at lower pH's.

(c) The increased concentration of HCl would also result in an increase in the number of Cl^- ions which surround the $Ru(bpy)_3^{2+}$ complexes. They are highly polarizable and hence can more easily relax the excited state of the complexes than water or ethanol molecules that are somehow restricted in rotation.

(d) The evaporation of the solvent molecules will leave gel pores filled with air if the pore shrinkage does not fully proceed. If each $Ru(bpy)_3^{2+}$ complex is just weakly interacting with the oxygen atoms of the silanol groups and/or siloxane chains of the gel network and also in part surrounded by O_2 and N_2 molecules, relaxation of the excited state can more easily take place than when the complexes are fully surrounded by solvent molecules that are restricted in rotation.

(e) If the evaporation of the solvent molecules leaves the gel pores vacant, the rotational movements of the excited $Ru(bpy)_3^{2+}$ complexes are also expected, allowing the excited state to be relaxed and resulting in the red shift as suggested by Avnir et al. for rhodamine 6G in silica gels.[34]

As far as the red shift of the fluorescence peak up to 200 °C is concerned, the explanations d and e above are the most probable if you take into account the decreased fluorescence efficiency observed with increasing drying temperature as will be discussed in section 4.4. It was also observed that the emission peak showed red shift when the as-deposited film was placed under vacuum (5×10^{-1} Torr) for 30 min at room temperature, whereby some portion of the solvent may be removed from the gel pores. As mentioned in section 3.3, we observed for the first time the distinct red shift of the $Ru(bpy)_3^{2+}$ fluorescence peak during drying. Castellano et al.[14] and Matsui et al.[15] observed the blue shift of $Ru(bpy)_3^{2+}$ in the sol-to-wet gel-to-xerogel conversion process in bulk silica gels; Matsui et al.[15] observed for some samples a very slight red shift during drying at room temperature, but the shift was as small as 2 nm, which is much smaller than that observed in the present study (13 nm). McKiernan et al.[29] observed a similar trend for bulk silica and aluminosilicate gels doped with $ReCl(CO)_3(bpy)$. In all of these previous works the drying of the gels was conducted at room temperature. Drying at room temperature cannot fully release the solvent molecules from gels, especially those chemically bonded to silanol groups. This can only cause the blue shift under drying. In contrast, because of the drying at higher temperatures, even the chemically bonded solvent molecules gradually evaporate, leaving the complexes in relatively vacant gel pores, which can cause the red shift of the fluorescence peak.

At temperatures higher than 200 °C, the blue shift of the fluorescence peak was again observed. A noticeable decrease of Si−OH was observed above this temperature (Figure 8), which results from the condensation reaction between the silanol groups. Two possible explanations can be made for this blue shift. (1) At this stage, because of the condensation reaction, the gel pores are collapsed, and the complexes are almost fully entrapped in the gel network, totally surrounded by the rigid gel network. This leads to a blue shift of the emission via rigidochromism. (2) Because of the condensation reaction, less polarizable Si−O−Si increases in number while more polarizable Si−OH decreases, leading to less chance for the excited state to be relaxed.

4.3. Fluorescence Lifetime. In the present study, bimodal lifetime was employed to fit the decay data to a theoretical curve. Bimodal lifetime has been observed by several authors in sol−gel-derived bulk silica gels doped with organic or organometallic fluorescent molecules and complexes.[14,35] It is possible to think that the fluorescent molecules or complexes occupy at least two different sites in gels, but the exact reason for the bimodal lifetime is still unknown.

Fluorescence lifetime drastically increased on drying at 100 °C as shown in Table 1. Two factors are considerd to cause the increased lifetime. First, as suggested by Caspar et al.[36] in the study on the decay of MLCT excited states, high frequency ν(O−H) modes around 3400 cm^{-1} can play a role as energy acceptors in nonradiative decay.[31] Since the sharp decrease of 3400 cm^{-1} infrared absorption bands at 100 °C as in Figure 8 is closely related to the solvent evaporation, the increase in lifetime can be attributed to the decrease in the ν(O−H) modes as energy acceptors in nonradiative decay.

Second, the effect of the entrapment of the complexes in the gel network seems to be present as in the case of the entrapment in zeolites and cellulose acetates.[37−39] Lumpkin et al.[37] and Maruszewski et al.[38,39] observed that the lifetime of the $Ru(bpy)_3^{2+}$ complexes increased when they were entrapped in

zeolites or cellulose acetates. They modeled the temperature dependence of the excited lifetime by a kinetic equation with two thermal terms corresponding to the so-called, thermally induced fourth ^{3}MLCT state, lying above the lowest lying MLCT state and below the ligand field state (LF state, metal-centered d-d state). The thermal population of the LF state (d-d excited state) can mask the decay of the excited state via the fourth ^{3}MLCT state, leading to rapid and efficient nonradiative decay as schematically illustrated in Figure 9b. When the complexes are entrapped in zeolites or cellulose acetates, they thought the energy gap between the low-lying ^{3}MLCT states and the LF state increases due to the restrictions imposed by the fixed size of the cage. This increase in the energy gap renders the LF state thermally inaccessible to the excited electrons, leading to the elimination of the decay through the d−d pathway. One can expect that this possibly happens also to the present samples, especially those dried at higher temperatures, where the gel pores are collapsed and the complexes are almost fully entrapped in the gel network. The absorption band ascribed to the metal-centered d−d transition, however, is not changed in energy with drying temperature for the present samples (Figure 2). Therefore this explanation on the increased lifetime appears to be not very probable.

4.4. Fluorescence Efficiency. It is known that O_2 gas deactivates the excited state of $Ru(bpy)_3^{2+}$, giving rise to quenching.[2,17,18,40,41] During drying, the silica gel films experience the evaporation of the solvent, which leaves the $Ru(bpy)_3^{2+}$ complexes in the open gel pores and makes them accessible to O_2 gas. This would yield the decreased fluorescence efficiency. As seen in Figure 5, the decrease in fluorescence efficiency with increasing drying temperature was significant up to 100 °C, where drastic solvent evaporation was evidenced by the IR spectra (Figure 8). This illustration on the change of the gel film and of the chemical state of the complex also agrees with what we have described on the basis of the fluorescence peak shift in section 4.2. Over 200 °C, where we thought pore collapse occurs, the fluorescence efficiency does not increase but remains almost constant. Probably even over 200 °C the collapse of the pores is not completed and the complexes are still accessible to O_2 gas.

4.5. Process of the Entrapment of $Ru(bpy)_3^{2+}$. On the basis of the above discussion, a possible model can be illustrated on the process of the entrapment of the $Ru(bpy)_3^{2+}$ complexes in the present silica coating films as shown in Figure 10. In the sol state, the $Ru(bpy)_3^{2+}$ complexes are surrounded by the solvent molecules, which are free to move or rotate upon excitation of the complexes (Figure 10a). In the as-deposited film, the complexes are surrounded by the solvent molecules which interact so strongly with the silanol groups of the gel network that they have restrictions somehow in rotation or movement (Figure 10b). Such restrictions depress the relaxation of the excited state of the complexes, resulting in the blue shift of the fluorescence peak.

When the films are dried at temperatures lower than 200 °C, the solvent in the gel pores evaporates, leaving the gel pores vacant somehow, and the complexes are weakly bonded to the gel network via direct interaction with the oxygen atoms of the silanol groups and/or siloxane chains or via chloride ions (Figure 10c). Because the complexes obtain more freedom of rotation and/or are surrounded by air molecules at this stage, the excited state can be relaxed to some extent, resulting in the red shift of the fluorescence peak. The complexes are now accessible to O_2 molecules, leading to the fluorescence quenching. The evaporation of the H_2O and C_2H_5OH molecules chemically bonded to the silanol groups decreases the amount of OH groups,

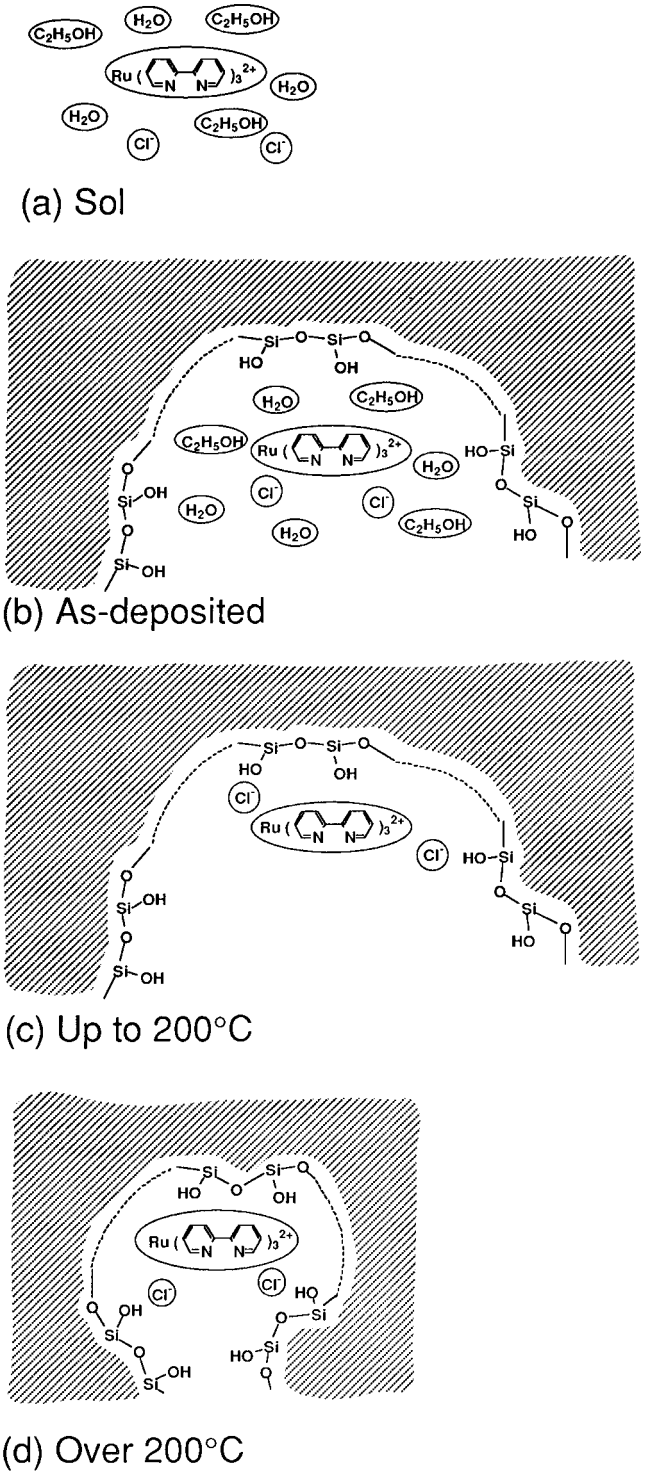

Figure 10. A possible illustration on the process of the entrapment of $Ru(bpy)_3^{2+}$ in the present silica gel film.

which can act as energy acceptors in nonradiative decay, giving rise to the increased fluorescence lifetime.

Over 200 °C condensation reactions between the silanol groups causes gel pores to collapse, and the complexes are almost fully entrapped in the gel network (Figure 10d). Because of decreased freedom, in other words, the immobilization, the complexes again experience rigidochromism, showing the blue shift of the fluorescence peak.

5. Conclusions

Silica gel films doped with tris(2,2′-bipyridyl)ruthenium(II) ($Ru(bpy)_3^{2+}$) complex were prepared by the sol−gel method,

and the fluorescence properties of the films were measured as a function of the drying temperature.

(1) The fluorescence peak attributed to the transition from the MLCT excited state to the ground state of $Ru(bpy)_3^{2+}$ showed blue shift on sol-to-gel film conversion, red shift up to 200 °C, and blue shift over 200 °C.

(2) The fluorescence lifetime increased and the fluorescence efficiency decreased with increasing drying temperature.

(3) A possible model has been proposed for the process of the entrapment of the complex during the film deposition and drying processes. In the as-deposited film, the complexes are surrounded by the solvent molecules that are interacting with the silanol groups of the gel network so strongly that the complexes exhibit rigidochromism in fluorescence. During drying up to 200 °C the solvents in the gel pores evaporate, which leaves the complexes weakly bonded to the gel network and surrounded by the air molecules, leading to the red shift of the fluorescence peak and fluorescence quenching by O_2 molecules. Over 200 °C the gel pores collapse via condensation reactions between the silanol groups, and the complexes are almost fully entrapped in the gel network, giving rise to the blue shift of the fluorescence peak.

Acknowledgment. We are in debt to Prof. Y. Ogata of the Institute of Advanced Energy, Kyoto University, and Dr. T. Uchino of the Institute for Chemical Research, Kyoto University, for FTIR measurements, Prof. T. Shimizu, Dr. M. Fujizuka, Mr. K. Fukui, and Mr. K. Susumu of the Division of Molecular Engineering, Faculty of Engineering, Kyoto University, for lifetime measurements, and Prof. S. Takahashi of the Institute for Chemical Research, Kyoto University, for fluorescence anisotropy measurements. H.K. thanks the Iwatani Naoji Foundation for their financial support. P.I. thanks the European Union for granting the fellowship in Japan.

References and Notes

(1) Carraway, E. R.; Demas, J. N.; DeGraff, B. A.; Bacon, J. R. *Anal. Chem.* **1991**, *63*, 337.

(2) MacCraith, B. D.; McDonagh, C.; O'Keefe, G.; Keyes, E. T.; Vos, J. G.; O'Kelly, B.; McGilp, J. F. *Analyst* **1993**, *118*, 385.

(3) MacCraith, B. D.; McDonagh, C.; O'Keefe, G.; McEvoy, A. K.; Butler, T.; Sheridan, F. R.; Proc. *SPIE-Int. Soc. Opt. Eng.* **1994**, *2288* (Sol-Gel Optics III), 518.

(4) Kiernan, P.; McDonagh, C.; MacCraith, B. D.; Mongey, K. *J. Sol-Gel Sci. Technol.* **1994**, *2*, 513.

(5) Slama-Schwok, A.; Avnir, D.; Ottolenghi, M. *J. Am. Ceram. Soc.* **1991**, *113*, 3984.

(6) O'Regan, B.; Grätzel, M. *Nature* **1991**, *353*, 737.

(7) Nazeeruddin, M. K.; Liska, P.; Moser, J.; Vlachopoulos, N.; Grätzel, M. *Helv. Chim. Acta* **1990**, *73*, 1788.

(8) Zyss, J.; Dhenaut, C.; Chauvan, T.; Ledoux, I. *Chem. Phys. Lett.* **1993**, *206*, 409.

(9) Avnir, D.; Kaufman, V. R.; Reisfeld, R. *J. Non-Cryst. Solids* **1985**, *74*, 395.

(10) Zink, J. I.; Dunn, B. S. *J. Ceram. Soc. Jpn.* **1991**, *99*, 878.

(11) Reisfeld, R. *J. Non-Cryst. Solids* **1990**, *121*, 254.

(12) Dvorak, O.; DeArmond, M. K. *J. Phys. Chem.* **1993**, *97*, 2646.

(13) Reisfeld, R.; Brusilovsky, D.; Eyal, M.; Jorgensen, C. *Chimia* **1989**, *43*, 385.

(14) Castellano, F. N.; Heimer, T. A.; Tandhasetti, M. T.; Meyer, G. J. *Chem. Mater.* **1994**, *6*, 1041.

(15) Matsui, K.; Sasaki, K.; Takahashi, N. *Langmuir* **1991**, *7*, 2866.

(16) Innocenzi, P.; Kozuka, H.; Yoko, T. *J. Non-Cryst. Solids* **1996**, *201*, 26.

(17) Juris, A.; Balzani, V.; Barigelletti, F.; Campagna, S.; Belser, P.; Von Zelewsky, A. *Coord. Chem. Rev.* **1988**, *84*, 85.

(18) Cook, M. J.; Lewis, A. P.; McAuliffe, G. S. G.; Skarda, V.; Thomson, A. J.; Glasper, J. L.; Robbins, D. J. *J. Chem. Soc., Perkin Trans. 2* **1984**, 1293.

(19) Belser, P.; Daul, C.; Von Zelewsky, A. *Chem. Phys. Lett.* **1981**, *79*, 596.

(20) Ferguson, J.; Herren, F. *Chem. Phys.* **1983**, *76*, 45.

(21) Kober, E. M.; Meyer, T. J. *Inorg. Chem.* **1982**, *21*, 3967.

(22) Galeener, F. G. *Phys. Rev. B* **1979**, *19*, 4292.

(23) Almeida, R. M.; Guitton, T. A.; Pantano, G. C. *J. Non-Cryst. Solids* **1990**, *121*, 193.

(24) Almeida, R. M.; Goncalves, M. C.; Grilo, J. L. *Mater. Sci. Forum* **1988**, *32-33*, 427.

(25) Gleria, M.; Minto, F.; Beggiato, G.; Bortolus, P. *J. Chem. Soc., Chem. Commun.* **1978**, 285.

(26) Durham, B.; Caspar, J. V.; Nagle, J. K.; Meyer, T. J. *J. Am. Chem. Soc.* **1982**, *104*, 4803.

(27) Wrighton, M.; Morse, D. L. *J. Am. Chem. Soc.* **1974**, *96*, 998.

(28) Giordano, P. J.; Wrighton, M. S. *J. Am. Chem. Soc.* **1979**, *101*, 2888.

(29) McKiernan, J.; Pouxviel, J. C.; Dunn, B.; Zink, J. I. *J. Phys. Chem.* **1989**, *93*, 2129.

(30) Kim, H.-B.; Kitamura, N.; Tazuke, S. *J. Phys. Chem.* **1990**, *94*, 7401.

(31) Meyer, T. J. *Pure Appl. Chem.* **1986**, *58*, 1193.

(32) Milder, S. J.; Gold, J. S.; Kliger, D. S. *J. Phys. Chem.* **1986**, *90*, 548.

(33) Ferguson, J.; Krausz, E. *Inorg. Chem.* **1987**, *26*, 1383.

(34) Avnir, D.; Levy, D.; Reisfeld, R. *J. Phys. Chem.* **1984**, *88*, 5956.

(35) Narang, U.; Wang, R.; Prasad, P. N.; Bright, F. V. *J. Phys. Chem.* **1994**, *98*, 17.

(36) Caspar, J. V.; Sullivan, B. P.; Kober, E. M.; Meyer, T. J. *Chem. Phys. Lett.* **1982**, *91*, 91.

(37) Lumpkin, R. S.; Kober, E. M.; Worl, L. A.; Murtaza, Z.; Meyer, T. J. *J. Phys. Chem.* **1990**, *94*, 239.

(38) Maruszevski, K.; Strommen, D. P.; Kincaid, J. R. *J. Am. Chem. Soc.* **1993**, *115*, 8345.

(39) Maruszevski, K.; Kincaid, J. R. *Inorg. Chem.* **1995**, *34*, 2002.

(40) Carraway, E. R.; Demas, J. N.; DeGraff, B. A. *Langmuir* **1991**, *7*, 2991.

(41) Demas, J. N.; Diemente, D.; Harris, E. W. *J. Am. Chem. Soc.* **1973**, *95*, 6864.